Enhanced Field Calculation for HVDC GIS

F. Messerer, W. Boeck, H. Steinbigler and S. Chakravorti *

1. INTRODUCTION

The high reliability and compactness achieved by compressed gas insulation in HVAC systems, has led to the development of HVDC Gas Insulated Substations (GIS). As in case of HVAC GIS, the basic insulation components of HVDC GIS are SF_6 gas and solid spacers. In this respect, it has been recognized that the breakdown strength of GIS is mainly influenced by spacers. For HVAC GIS, the problems related to spacers can be eliminated to a great extent by a careful electric stress control design[1−3]. However, for HVDC GIS stress control designs based on dielectric interfaces with no trapped charges are not valid, since charges get accumulated on spacer surfaces which distort the designed Laplacian field distribution. In this context, it is also kept in mind that SF_6 insulation is very sensitive to local enhancement of electric field. According to this surface charge accumulation and its effects in HVDC GIS have been studied in various aspects by several researchers[4−11]. In order to improve the dielectric performance of epoxy spacers by properly shaping the gas-dielectric interfaces, studies on electric field optimization along the profile of the gas-dielectric interface in gas insulated systems have been reported in literature[12,13]. For HVDC GIS, investigations on the effects of spacer shapes on flashover characteristics have also been carried out[14]. Since, in contrary to HVAC GIS, the electric field distribution at steady-state in HVDC GIS is mainly controlled by the conductivity κ of the dielectric media, studies on the influence of volume and surface resistivities on the electric field distribution around GIS spacers have been done[15]. It has also been suggested that a conducting coating on the spacer surface may help to obtain a controlled current density on the spacer surface and also to reduce the surface charge accumulation[16].

This paper reports about the results of detailed numerical studies on electric field distribution around a standard 145 kV epoxy spacer for use in HVDC GIS. The field calculations are based on Boundary Element Method (BEM)[17] with necessary modifications in boundary conditions. Firstly, the effects of various parameters

*F. Messerer, W. Boeck, H. Steinbigler, Institute of High Voltage Engineering and Electric Power Transmission, Technical University Munich, Germany. S. Chakravorti, Jadavpur University Calcutta, India.

such as volume resistivity, uniform and non-uniform surface resistivities and accumulated surface charges on field distribution have been determined. Subsequently, possible ways of optimizing electric field distribution around the spacer have been discussed.

2. METHOD OF FORMULATION

For numerical field analysis, accurate simulation of boundaries is critically important, as the knowledge of field distribution on or near the electrode and insulator boundaries is of practical significance. Herein lies the inherent advantage of employing BEM, which divides the electrode and insulator surface into suitable number of surface or boundary elements. The charge distribution on these boundary elements is determined by imposing the appropriate boundary conditions.
It has been established[18], so long as true charges exist only on the boundaries, integral methods can be employed for numerical field calculation. Hence, from the consideration of practical aspects of HVDC GIS, the following features have been incorporated in the BEM based formulation of the dielectric - dielectric boundary conditions:

- user defined volume resistivities at any node
- user defined surface resistivity between any two nodes
- user defined value of accumulated surface charge at any node

As a result, instead of purely capacitive, capacitive - resistive field calculations with complex values of potentials and charges[19,20] have been carried out as detailed below. At any node i on the dielectric - dielectric boundary,

$$\bar{\varepsilon}_1 \bar{E}_{1n}(i) - \bar{\varepsilon}_2 \bar{E}_{2n}(i) = \bar{\sigma}_s(i) + \bar{\sigma}_a(i) \tag{1}$$

where $\sigma_a(i)$ is the value of accumulated surface charge density at any node i, ε is the permittivity and $\sigma_s(i)$ is found from the general condition of the current density vector at the node i[21] as follows:

$$\bar{J}_{1n}(i) - \bar{J}_{2n}(i) + \Delta \bar{J}_s(i) + \frac{\partial \bar{\sigma}_s(i)}{\partial t} = 0 \tag{2}$$

or

$$\frac{\bar{E}_{1n}(i)}{\rho_{v1}} - \frac{\bar{E}_{2n}(i)}{\rho_{v2}} + \Delta \bar{J}_s(i) + j\omega \bar{\sigma}_s(i) = 0 \tag{3}$$

where $\rho_v(i)$ is volume resistivity at any node i and suffixes 1 and 2 denote dielectric media 1 and 2 respectively. In equation (3) the surface current density term $\Delta J_s(i)$ can be expanded as mentioned in[22]. Combining equations (1), (2) and (3) it may be written as

$$\frac{2[\bar{\varepsilon}_1(i) - \bar{\varepsilon}_2(i)]}{\bar{\varepsilon}_1(i) + \bar{\varepsilon}_2(i)} \bar{E}_n(i) - \frac{2j}{\omega S(i)[\bar{\varepsilon}_1(i) + \bar{\varepsilon}_2(i)]} \cdot$$
$$\left[\bar{\Phi}(i)\left\{\frac{1}{R(i)} + \frac{1}{R(i+1)}\right\} - \frac{\bar{\Phi}(i+1)}{R(i+1)} - \frac{\bar{\Phi}(i-1)}{R(i)}\right] + \frac{\bar{\sigma}(i)}{\varepsilon_0} = \frac{2\bar{\sigma}_a(i)}{\bar{\varepsilon}_1(i) + \bar{\varepsilon}_2(i)} \tag{4}$$

where

$$\bar{\varepsilon}_x(i) = \varepsilon_0 \varepsilon_{rx} + \frac{1}{j\omega \rho_{vx}(i)} \tag{5}$$

$\omega = 2\pi$f and f is the frequency. $E_n(i)$ is the normal component of electric field intensity at the node i by charge densities at all the nodes[17,23]. σ(i) is the charge density and Φ(i) is the potential at the node i, respectively. $S(i)$ is a small area, $R(i)$ and $R(i+1)$ are surface resistances around node i. The method of calculation of $S(i)$, $R(i)$ and $R(i+1)$ are described in[20].

2.1. Steady State Condition of Surface Charge Accumulation

In HVDC GIS, free charges are generated primarily by field emission at electrode surfaces. These charges move along the electric flux lines from the gas side onto the spacer surface. The trapped charges could move along the spacer surface only if the surface conductivity provides adequate mobility. Hence if the surface resistivity is high, charge accumulation on spacer surface takes place. The charge accumulation reduces E_{1n} at gas side, while it enhances E_{2n} at the spacer side gradually until the steady state is reached[5,9], when

$$\bar{E}_{1n}(i) = 0 \tag{6}$$

BEM based formulation of the boundary condition given in equation (6) has also been implemented as follows. Considering the orientation of the normal vector to the gas side at any node i on the spacer-gas boundary, it may be written that

$$\bar{E}_{1n}(i) = \bar{E}_n(i) + \frac{\bar{\sigma}(i)}{2\varepsilon_0} \tag{7}$$

Thus, replacing equation (4) by (7) and then solving for σ(i), the field distribution around solid spacer at the steady-state condition of surface charge accumulation may be calculated.

2.2. Software Xtwin

A complete user-friendly, interactive software named *Xtwin* based on the BEM formulations described above has been developed for axi-symmetric field calculation employing two types of elements, viz. straight line and elliptic arc elements, and considering a linear basis function for the description of charge distribution along an element between a pair of nodes. A graphical interface starts the various calculations and controls the pre- and postprocessing. The results can be presented in 2D-Plots or with a special visualization tool - which is based on VRML - as 3D-Plots. The voltage or field distribution is shown in different colors (see fig.1). All results presented in this paper are obtained using this software *Xtwin*.

3. APPLICATION EXAMPLE

The application example for the investigations is a standard spacer manufactured by SIEMENS for Gas Insulated Substations used in 145 kV systems. The simulation

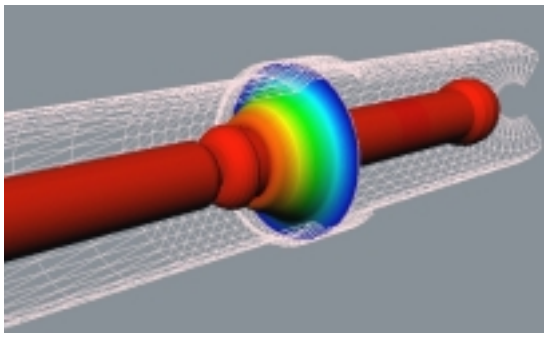

Fig. 1. 3D Modell of the system

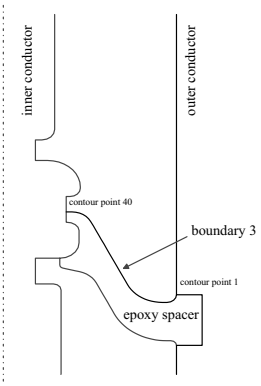

Fig. 2. 2D Modell of the spacer

model (fig. 1) shows the inner conductor, the spacer and the outer conductor of such a system.

For the field calculation the geometry has to be described in a 2D-axisymmetric system. Figure 2 shows the details of the spacer. The results are only shown for the convex side of the spacer (defined as boundary 3). The results for the concave side are nearly the same. All the calculations are made with a normalized voltage of $U = 1.0$. The results are given in 1/m.

4. CALCULATIONS

4.1. Influence of Surface Resistivity

One possible way to improve the field distribution of an HVDC GIS system is to change the surface conditions by using a conducting coating[15,16]. With the BEM-program *Xtwin* several different types of surface resistivity can be calculated. Investigations are made with uniform, non-uniform and non-linear surface resistivity. The calculations are made without influence of volume resistivity, that means with a fixed value of $\rho_{vol} = 10^{20}\Omega m$.

4.1.2. uniform coating

The influence of a constant surface resistivity on the field distribution has been investigated. The resistivity has been varied from $10^{10}\Omega$ to $10^{20}\Omega$. A spacer with a surface resistivity of $10^{10}\Omega$ is labeled with s10.

The results show that there is no difference between $10^{10}\Omega$ to $10^{15}\Omega$. A coating with this surface resistivity improves the field distribution compared to the uncoated spacer ($\rho_{sur} > s18$). The peak value of the normal field stress is considerably reduced from 23 1/m down to 17 1/m (fig. 3). The tangential field distribution (fig. 4) is more homgeneous than without a coating, but the field is enhanced at the high voltage side.

The resultant field distribution (fig. 5) is improved using a conducting coating with a surface resistivity between 10^{10} to $10^{15}\Omega$. The field is slightly enhanced at the high voltage side of the spacer.

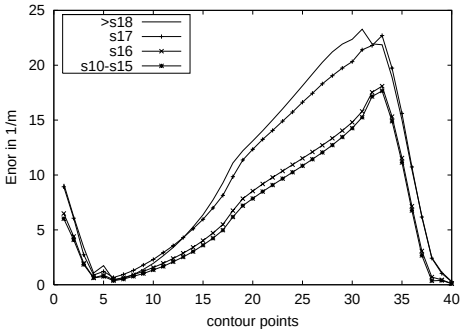

Fig. 3. Influence of uniform coating on E_{nor}

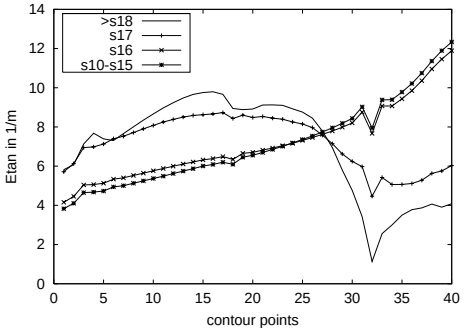

Fig. 4. Influence of uniform coating on E_{tan}

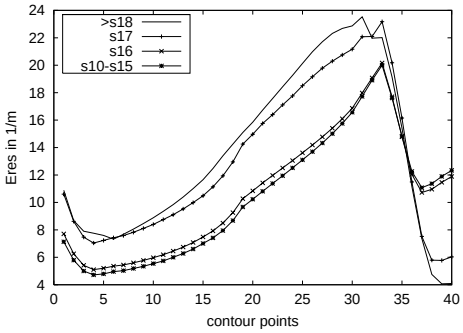

Fig. 5. Influence of uniform coating on E_{res}

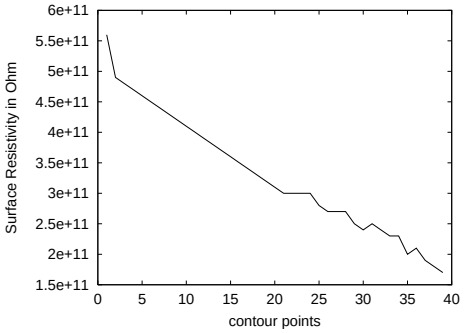

Fig. 6. Surface resistivity distribution

4.1.3. non-uniform coating

The tangential field has been increased at the high voltage side of the spacer (fig. 4). In order to obtain better results it is useful to use a non-uniform coating on the surface of the spacer. The current density can be described as a function of the radius r. If the resistance load is reduced, the local potential and therefore the local electric field will be decreased.

$$E = j \cdot \rho = \frac{I}{2\pi r} \cdot \rho \tag{8}$$

For this non-uniform coating each contour point can be defined with a certain surface resistivity. The distribution is shown in fig. 6.

Using such a coating the resistance and therefore the potential drop is rised at the grounded conductor (contour point 1). Because the total potential between the electrodes is constant ($U = \int Eds = const$) the field stress is reduced at the the high voltage electrode. With that special coating it is possible to achieve a homegeneous tangential field distribution along the whole spacer (fig. 8). The normal and the resultant field stress is still lower than without coating (fig. 7,9).

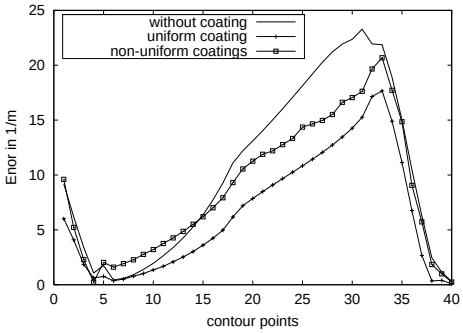

Fig. 7. Influence of non-uniform coating on E_{nor}

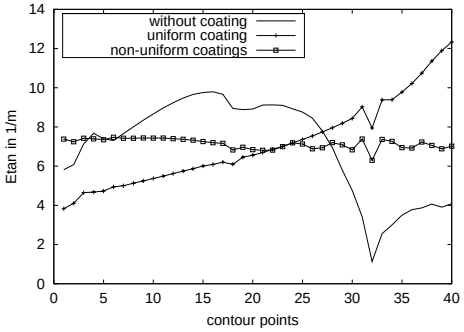

Fig. 8. Influence of non-uniform coating on E_{tan}

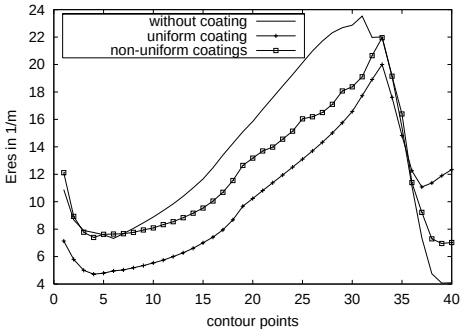

Fig. 9. Influence of non-uniform coating on E_{res}

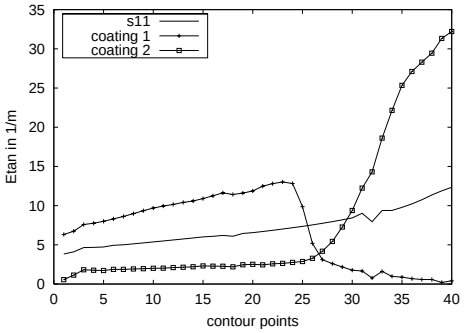

Fig. 10. Influence of non-linear coating on E_{tan}

Using a non-uniform coating may be a promising way to improve the field distribution of HVDC-GIS-systems.

4.1.4. non-linear coating

In the case of non-linear coatings, that means the resistance is dependent on the field stress the field distributions are different. For the calculations a dependence of ρ_{sur} on E_{tan} is realised. The calculations were made iterativly.

E_{tan} in 1/m	2	4	6	8	10	12	14
ρ_{sur1} in $10^{11}\Omega$	128	64	32	16	8	4	1
ρ_{sur2} in $10^{11}\Omega$	2	4	6	8	10	12	14

TABLE I

NON-LINEAR SURFACE COATING

In table I two possible dependencies are shown. The surface resistivity distribution ρ_{sur1} is decreasing with rising field stress. That means at the high voltage side

of the spacer (with higher field stresses) the resistance is reduced and therefore the tangential field is also reduced (fig. 10) similar to section 4.1.3. The tangential field is considerably reduced at the high voltage side but the normal and resultant field stress is enhanced (fig. 11, 12). For practical use such a coating with a non-linear surface resistivity distribution is not an optimum solution.

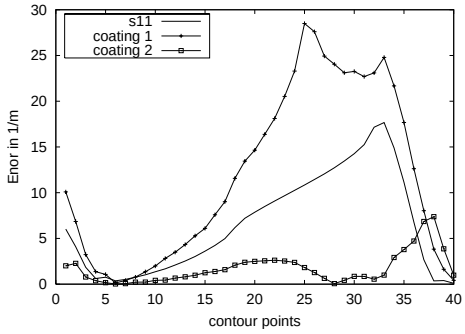

Fig. 11. Influence of non-linear coating on E_{nor}

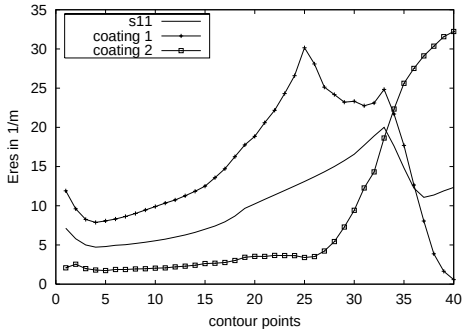

Fig. 12. Influence of non-linear coating on E_{res}

Regarding the second non-linear surface resistivity distribution in table I, with rising resistance due to rising field stress, different things can be detected. Although the normal field (fig. 11) is perfectly reduced the tangential and resultant field stress is dramatically enhanced at the high voltage side of the spacer (fig. 10, 12). The results of the investigations concerning non-linear surface resistivity show that this is not a promising way to optimize an HVDC-GIS-system.

4.2. Influence of Volume Resistivity

Investigations on the influence of volume resistivity on the field distribution are made. That means the dielectric conditions of the epoxy of the spacer are changed.

4.2.1. without surface resistivity

The first calculations are carried out without surface resistivity, that means $\rho_{sur} = 10^{20}\Omega$. The values of volume resistivity are varied from $\rho_{vol} = 10^{10}\Omega m$ (v10) to $\rho_{vol} = 10^{20}\Omega m$ (v20).

The figures 13,14 show that there is nearly no influence of volume resistivity on the field distribution. But the tangential field stress is enhanced compared to a normal spacer (v20). These calculations show that changing the dielectric conditions of the spacer does not improve the electric field distribution.

4.2.2. with surface resistivity

As shown in section 4.1.2. a constant surface resistivity improves the field distribution of HVDC-GIS-spacers. Additional investigations are made concerning the influence of volume resistivity in addition to a constant surface resistivity. In fig. 15,16 you can see the different field distributions of a standard spacer (s20v20) compared with different volume resistivities (s11vXX). Using a constant surface

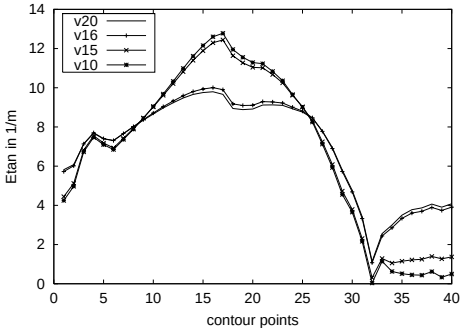

Fig. 13. Influence of volume resistivity on E_{tan}

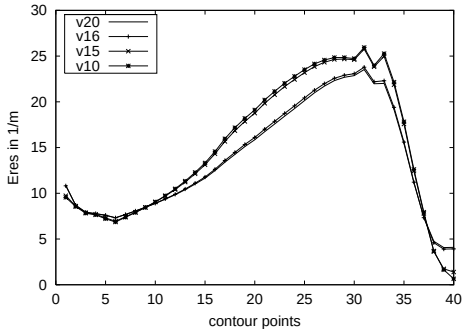

Fig. 14. Influence of volume resistivity on E_{res}

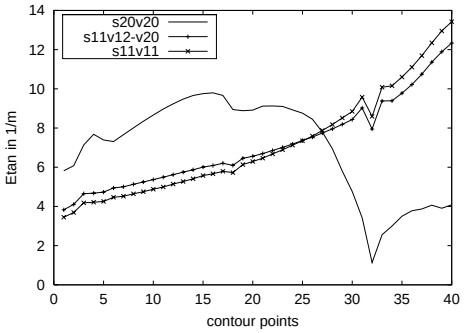

Fig. 15. Influence of volume resistivity on E_{tan}

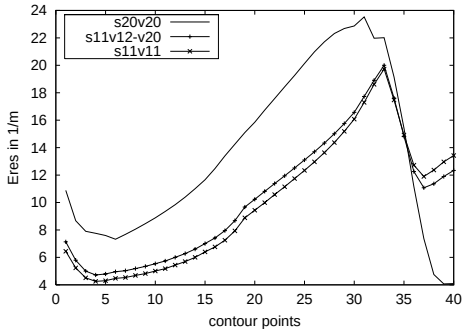

Fig. 16. Influence of volume resistivity on E_{res}

resistivity of $\rho_{sur} = 10^{11}\Omega$ the field distribution is similar to 4.1.2. The changing of the volume resistivity does not have a significant influence on the field distribution. Therefore changing the dielectric conditions of a spacer is not a possible way to improve the field distribution of HVDC-GIS-systems.

4.3. With Boundary Condition $E_n = 0$

As mentioned in 2.1. a charge accumulation on the surface of the spacer influences the field distribution. Calculations are made with an additional boundary condition $E_n = 0$ to simulate a steady state condition of a fully charged spacer.

Fig. 17 shows the influence on the tangential field distribution. The field is dramatically enhanced up to 29 1/m. The main field stress occurs at the high voltage side of the spacer. The resultant field stress (fig. 18) shows again that the field is lowered at the grounded side of the spacer and enhanced at the high voltage side. For an uncoated spacer (s20) such a high tangential field stress may lead to surface flashover. Therefore it is not applicable to use a standard, uncoated spacer for HVDC GIS systems.

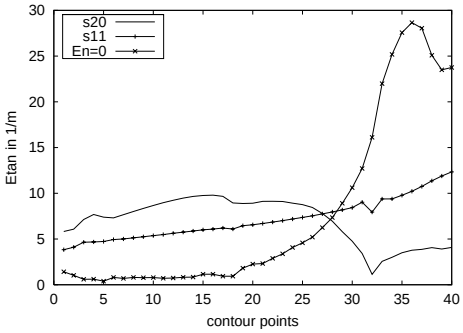

Fig. 17. E_{tan} with boundary condition $E_n = 0$

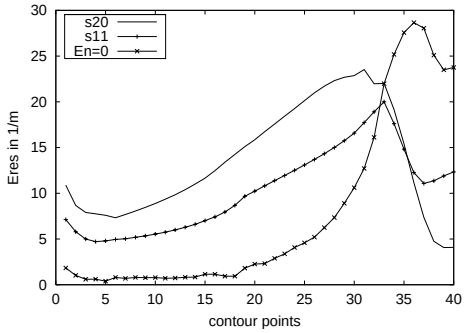

Fig. 18. E_{res} with boundary condition $E_n = 0$

4.4. With Surface Charge

Regarding section 4.3. the boundary condition $E_n = 0$ is the final state for a fully charged spacer. But from the beginning of the charging to the end different field distributions can be detected. Therefore calculations with defined values of surface charge densities are made to investigate the influence of the charge on the field distribution.
The calculations are made with a constant charge density. The results are shown for a positive and negative charge density of $300\frac{pC}{m^2}$.

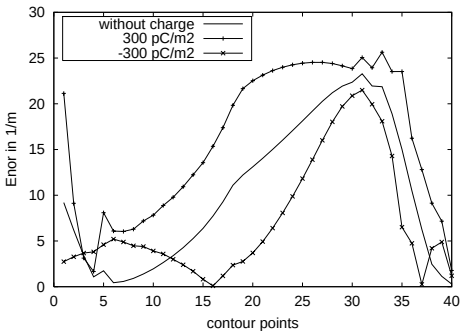

Fig. 19. Influence of surface charge on E_{nor}

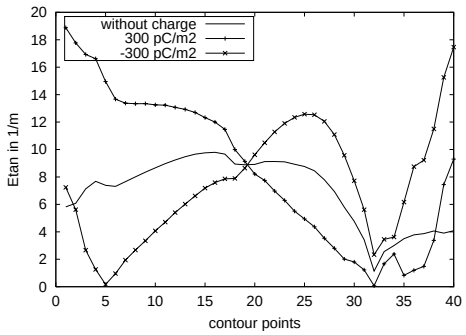

Fig. 20. Influence of surface charge on E_{tan}

Fig. 19 shows the normal component of the field distribution. A positive charge layer enhances and a negative reduces the field distribution, but no critical points can be detected. For the tangential field (fig. 20) different results are obtained. The positive charge layer enhances the field at the grounded side of the spacer (contour point 1). For a negative charge the field is enhanced at the high voltage side with two maxima (contour point 25 and 40). The resultant field (fig. 21) for a positive charge layer shows that a maximum appears at the grounded side and the complete field distribution is enhanced compared to the normal distribution

without charge.

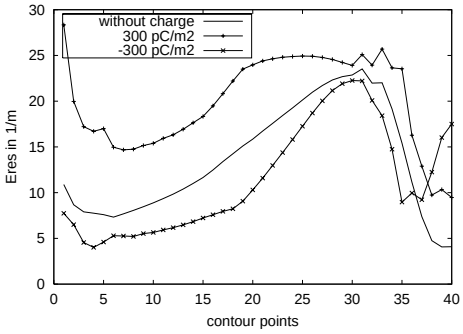

Fig. 21. Influence of surface charge on E_{res}

A negative surface charge density reduces the resultant field except at the high voltage side of the spacer (contour point 37-40). The final state is a fully charged spacer with a negative layer like shown in fig. 18. A charge density of $300\frac{pC}{m^2}$ is an intermediate state in the transient charging mechanism.

5. CONCLUSIONS

Enhanced field calculations for HVDC GIS systems are made and discussed in this paper.

- The influence of surface resistivity on the field distribution is investigated.
  - A uniform coating with a resistance of about $10^{11}\Omega$ improves the field distribution.
  - A non-uniform coating with a decreasing resistance due to increasing voltage is a promissing way to improve the field distribution.
  - A non-linear coating, that means the resistance is dependent on the field stress is not an optimum solution for HVDC GIS systems.
- Volume resistivity does not have significant influence on the field distribution. Changing the dielectric conditions of the spacer is not a possible way to improve the field distribution.
- Investigations with the additional boundary condition $E_n = 0$ show the steady state field distribution of a fully charged spacer. The electric field is dramatically enhanced at the high voltage side of the spacer.
- Calculations with surface charge can show the intermediate state of the field in the transient charging mechanism.

ACKNOWLEDGMENTS

Dr. S. Chakravorti would like to convey his thanks to the Alexander von Humboldt-Stiftung, Germany for granting him research fellowship to take part in the development work of *Xtwin* at the Institute of High Voltage Engineering and Electric Power Transmission, Technical University, Munich, Germany.

REFERENCES

1. C.M. Cooke, J.G. Trump, Post type support spacers for compressed gas-insulated cables, IEEE Trans. on PAS, Vol.92, 1973, pp. 1441-1448
2. J.R. Laghari, A.H. Qureshi, Surface flashover of spacers in compressed gas insulated systems, IEEE Trans. on EI, Vol.16, 1981, pp. 373-387

3. Y.Yamano, S. Kobayashi, Y. Takahashi, Improvement of flashover strength and reduction of surface charge induced field enhancement of insulating material, IEEE Trans. on EI, Vol.21, 1986, pp. 189-195
4. K. Nakanishi, A. Yoshioka, Y. Arahata, Y. Shibuya, Surface charging on epoxy spacer at DC stress in compressed SF6 gas, IEEE Trans. on PAS, Vol.102, 1983, pp. 3919-392
5. S. Sato, W.S. Zaengl and A. Knecht, A numerical analysis of accumulated surface charge on dc epoxy resin spacer, IEEE Trans. on EI, Vol.22, 1987, pp. 333-340
6. S.I. Bektas, Pacio-temporal development of surface charges on spacers stressed with dc voltages, IEEE Trans. on EI, Vol.25, 1990, pp. 515-520
7. S.E. Cherukupalli, K. Tsuruta and K.D. Srivastava, Mechanism of prebreakdown spacer charging in non-uniform fields under unidirectional voltages, IEEE Trans. on EI, Vol.25, 1990, pp. 642-654
8. T. Nitta, K. Nakanishi, Charge accumulation on insulating spacers for HVDC GIS, IEEE Trans. on EI, Vol.26, 1991, pp. 418-427
9. T. Jing, Surface charge accumulation - An inevitable phenomenon in DC GIS, IEEE Trans. on DEI, Vol.2, 1995, pp. 771-778
10. CIGRE Working Group 15.03, Gas Insulation Properties in Case of VFT and DC Stress, CIGRE paper 15-201, Working Group 15.03, 1996
11. S. Chakravorti, Modified E-field analysis around spacers in SF6 GIS under DC voltages 11^{th} ISH London, 1999, Vol.2, pp. 91-94
12. N.G. Trinh, F.A.M. Rizk and C. Vincent, Electrostatic field optimization of the profile of epoxy spacers for compressed SF6 insulated cable, IEEE Trans. on PAS, Vol.99, 1980, pp. 2164-2174
13. K. Itaka, T.Hara, T.Misaki and H. Tsuboi, Improved Structure avoiding local field intensification on spacers in SF6 gas, IEEE Trans. on PAS, Vol.102, 1983, pp. 250-255
14. H.Lee, T. Egashira and M. Hara, Improvement of particle initiated dc flashover characteristics by using electrode and surface shapes in SF6 gas, Proc. of 3rd Int. Conf. on Prop. and Appl. of diel. Materials, Tokyo, 1991, pp. 529-532
15. F. Messerer, W. Boeck, Field Optimization of an HVDC-GIS-Spacer, Annual Report CEIDP, pp. 15-18, 1998, Atlanta
16. F. Messerer, W. Boeck, High resistance surface coating of solid insulating components for HDVC metal enclosed equipment, 11^{th} ISH London, 1999, Vol.4, pp. 63-66
17. Z. Andjelic, B. Krstajic, S. Milojkovic, A. Blaszcyk, H. Steinbigler, M. Wohlmuth Integral Methods for the Calculation of Electric Fields, Scientific Series of the International Bureau, Vol. 10, Forschungszentrum Jülich GmbH, Germany, 1992
18. T. Takuma, T.Kawamoto and H. Fujinami, Charge Simulation Method with complex fictitious Charges for Calculating Capacitive-Resistive fields, IEEE Trans. on PAS, Vol.100, 1981, pp. 4665-4672
19. S. Chakravorti, H. Steinbigler, Capacitive-Resistive Field Calculation around a HV Insulator using Boundary Element Method, 10^{th} ISH Montreal, 1997, Vol.3, pp. 49-52
20. S. Chakravorti, P.K. Mukherjee, Power frequency and impulse field calculation around a HV insulator with uniform or non-uniform surface pollution, IEEE Trans. on EI, Vol.28, 1993, pp. 43-53
21. H. Singer, Feldberechnung mit Oberflächenleitschichten and Volumenleitfähigkeit der Isolation, ETZ-Archiv, Bd 3, H8, 1981, pp. 265-267
22. S. Chakravorti, H. Steinbigler, Capacitive-resistive field calculation on HV bushings using the boundary element method, IEEE Trans. on DEI, Vol.5, 1998, pp. 237-244
23. F. Gutfleisch, H. Singer, K. Foerger and J.A. Gomollon, Calculation of HV fields by mean of the boundary element method, IEEE Trans. on PWRD, Vol.9, 1994, pp. 743-749